

IMPACT OF INJECTION ERROR ON EUV FEL PERFORMANCE IN AN APL-BASED BEAMLINE

M. Miceski^{*1,2}, M. Matys¹, A. Whitehead^{1,2}, P. V. Sasorov¹, X. Wu³,
J. Vieira³, A. Jancarek^{1,2}, A. Molodozhentsev¹

¹The Extreme Light Infrastructure ERIC, Dolní Břežany, Czech Republic

²Czech Technical University in Prague, FNSPE, Prague, Czech Republic

³Instituto Superior Técnico, Lisbon, Portugal

Abstract

Recent advances in laser-plasma accelerators (LPAs) have generated high-quality electron beams characterized by high peak currents and low emittance, making them suitable for compact, next-generation free-electron lasers (FELs). However, variations in laser performance from shot to shot cause mismatches in position and angle at the injection point, complicating efficient beam transport and stable FEL operation. To preserve the electron bunch quality during beam propagation through the transport system, an active plasma lens (APL) can be used as part of the capture mechanism. This report investigates how injection errors influence electron beam properties along the beamline and their subsequent effect on FEL radiation in the extreme-ultraviolet (EUV) range. The results demonstrate an acceptable range of injection errors and emphasize the strengths and limitations of APL as capture system for optimal FEL performance. This work emphasizes the potential of APL technology to develop compact FELs and improve LPA beam applications. Such progress is vital for future FEL facilities at ELI ERIC in the Czech Republic and for the EuPRAXIA project.

INTRODUCTION

Laser-plasma accelerators provide accelerating gradients that are orders of magnitude higher than those achievable with conventional RF linacs, allowing much more compact configurations for generating high-energy electron beams. These beams are attractive candidates for driving next-generation free-electron lasers, capable of delivering ultrashort, high-brightness X-ray pulses. Such radiation sources open new opportunities for femtosecond-scale studies in physics, chemistry, biology, and materials science, as well as for applications in medicine and industry [1].

However, the intrinsically large energy spread and divergence of LPA-based beams present significant challenges for applications such as FELs. Active plasma lens provides an effective and compact solution, offering strong, azimuthally symmetric focusing with high field gradients that significantly reduce chromatic emittance growth. When operated in the linear regime, APL preserve beam emittance [2], making them particularly well suited for high-brightness applications. Their integration into the beamline is therefore a key step toward achieving efficient and reliable LPA-driven FEL operation. Laser pointing stability limits stable FEL

operation. These fluctuations translate into transverse and angular offsets of the electron beam, leading to charge loss at beamline apertures. This work presents a tolerance analysis of injection error and determines the threshold values required to keep saturation within the undulator.

FEL FRAMEWORK

Undulator Configuration

The undulator section under consideration consists of two consecutive SwissFEL-type U19 modules [3], each with an undulator period of 19 mm and a length of 2 m, resulting in a total interaction length of 4 m. The beam is matched at the entrance of the undulator such that a beam waist is formed at the center of the 4 m section, minimizing the average transverse beam size throughout the undulator section. This matching condition is essential for maintaining strong FEL coupling and efficient radiation gain. The undulator parameter, K_u , is a tunable quantity and can be adjusted in the range 1.2 to 1.9 by varying the size of the gap.

Electron Beam

The objective is to achieve saturation with the undulator section. To meet this requirement, the electron beam at the undulator entrance must satisfy specific conditions. For an electron beam of 300 MeV, these include an RMS slice normalized emittance below 0.4 mm mrad in both transverse planes, an RMS relative slice energy spread below 0.25% and a peak current of approximately 2.6 kA.

Laser-plasma accelerator technology has recently achieved significant advances that enable stable operation and the generation of high-quality electron beams. In this study, an electron beam of about 300 MeV is used, obtained with the shock-front injection method, as experimentally demonstrated [4, 5]. The initial electron beam is obtained using the OSIRIS PIC code [6]. Its projected parameters are as follows: the RMS divergence is 0.55 mrad (horizontal) and 0.71 mrad (vertical), and the RMS normalized emittance is 0.23 mm mrad (horizontal) and 0.37 mm mrad (vertical). The larger values in the vertical plane are because of the vertical laser polarization. The bunch charge is 24.71 pC, with a bunch length of 0.48 μm . These parameters indicate a high-quality electron beam for a beam obtained from laser-plasma acceleration.

* mihail.miceski@eli-beams.eu

ACTIVE PLASMA LENS AS A CAPTURE BLOCK

Electron beams generated from plasma sources typically exhibit relatively high divergence and non-negligible energy spread, leading to intrinsic emittance growth in the first drift [7]. Strong focusing is required to capture the beam but the high magnetic gradients introduce chromatic aberrations, which further increase the emittance and degrade beam quality [8]. In this section, a novel APL-based beamline is presented and compared with a conventional PQMs-based beamline. The comparison focuses on the ability of each system to preserve electron beam quality during transport. Despite significant advances in laser technology, laser pointing stability remains a limiting factor. These offsets are transferred to the generated electron beam, resulting in similar pointing and displacement errors. The errors are random and cannot be corrected along the beamline. As a result, they can lead to particle loss and degradation of beam quality. It is therefore important to analyze this effect and determine acceptable tolerance thresholds under which FEL saturation in the undulator can still be achieved.

Electron Beam Transport

In the case of a beamline based on a novel focusing system, the electron beam captured and focused with an active plasma lens [9, 10]. To limit emittance growth in the early stage of transport, the distance between the plasma source and the first focusing element must be minimized. In this setup, the APL is placed 15 cm downstream of the target, which is the minimum distance allowed by mechanical constraints. The APL operates with an argon gas fill in order to maintain a linear magnetic field profile, which supports the preservation of beam emittance [2, 11]. The lens has a length of 7 cm and a radius of approximately 1 mm, producing a magnetic field gradient of about 90 T/m. This configuration is currently under development at ELI ERIC. Downstream of the APL, there is space reserved for a chicane, followed by a matching section of three electromagnetic quadrupole magnets used to match the beam at the undulator entrance. The total beamline length is about 12 m. To mitigate the effects of beam halo generated by chromatic aberrations and space-charge forces, horizontal and vertical collimators are installed along the beamline. Their positions are chosen based on the phase-space evolution of the bunch. As the phase space rotates during transport, the collimators are placed where the halo is predominantly in position space. The placement is also guided by injection error studies, selecting locations where the beam offset is minimal (beam crosses the reference axis). In the APL-based beamline, two collimators are used. The first is located 2.5 m downstream of the source and has apertures of 0.21 mm (horizontal) and 0.28 mm (vertical), which removes a significant portion of the halo produced by chromatic effects. The second collimator is positioned 15 cm upstream of the undulator, with apertures of 0.40 mm (horizontal) and 0.22 mm (vertical), to further reduce the remaining halo.

In the case of a beamline based on a standard focusing system using permanent quadrupole magnets (PQMs), the overall layout remains the same [12]. The focusing section consists of two permanent quadrupole magnets followed by one electromagnetic quadrupole magnet. The first PQM is located 5 cm downstream of the target, with a gradient of 395 T/m, a length of 40 mm, and an aperture of 3 mm. It is followed by a 5 cm drift and a second PQM with a gradient of 225 T/m, a length of 50 mm, and an aperture of 6 mm. These magnets will be installed in vacuum. The third quadrupole magnet is placed 15 cm downstream. In the PQM-based beamline, the first collimator is located at the same position as in the APL-based beamline, with apertures of 0.32 mm (horizontal) and 0.22 mm (vertical). The second collimator is located 1.8 m upstream of the undulator entrance. This location is chosen where the beam offset is small and the phase-space orientation allows effective halo removal. The apertures of this collimator are 0.40 mm (horizontal) and 0.28 mm (vertical), respectively. In a beamline of this length, the electron bunch experiences strong space-charge forces, which gradually introduce an energy chirp along the bunch that is detrimental for FEL operation. To handle this, additional elements such as an active plasma dechirper or a dielectric structure are considered.

Analysis of Injection Error

In our setup, the laser is focused by an off-axis parabola at a distance of 2 m. Small angular fluctuations, on the order of microradians, therefore translate into micrometer-scale transverse offsets at focus. These are transferred to the electron beam, introducing pointing and displacement errors. Since these variations are random they cannot be corrected along the beamline and due to the very small apertures of the collimators significant charge can be lost. For the present study, the beam is assumed to be symmetric, such that offsets in different transverse directions lead to comparable effects. Therefore, a worst-case scenario is considered, where equal horizontal and vertical pointing shifts are applied. The laser pointing is varied from 0.5 μ rad to 2.5 μ rad in steps of 0.5 μ rad. This corresponds to electron beam offsets from 1 μ m to 5 μ m at the source. For each case, multi-particle tracking simulations with TraceWin code [13] are performed.

Fig. 1(a) shows the normalized emittance of the bunch at the entrance of the undulator. With increasing injection error, the beam arrives with higher emittance. This is related to the position of the collimators and the rotation of the bunch in phase space, where halo particles are not removed optimally, being overcut in one plane and undercut in the other. Fig. 1(b) shows the remaining bunch charge at the undulator entrance for different injection errors. A reduction in charge is observed due to losses at the collimators. In the PQMs-based beamline, the bunch orientation does not coincide with the optimal position (where the offset is minimal), leading to higher losses. An important observation is that particles within the resonance window are lost more slowly with increasing error in the APL-based beamline.

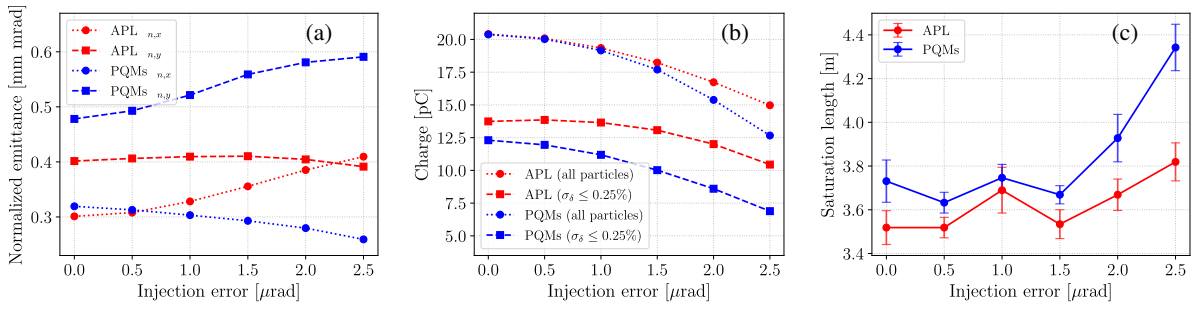


Figure 1: (a) Normalized transverse emittance (horizontal and vertical) at the undulator entrance as a function of injection error, shown for both beamline configurations. (b) Total charge remaining at the undulator entrance as a function of injection error for both beamline configurations. The charge within the resonance window (particles with kinetic energy deviation within 0.25% of the reference energy) is also shown. (c) Saturation length as a function of injection error, shown for both beamline configurations. The point represents the mean of the 12 shots with different shot noises and the error bar is standard error of the mean.

This indicates that resonant electrons remain more centered in the beam due to the more symmetric focusing.

FEL simulation

For each beam obtained at the undulator entrance from both beamline configurations, FEL simulations are performed to determine the saturation length. Time-dependent SASE FEL simulations were performed using the GENESIS code [14].

Fig. 1(c) shows the saturation length as a function of injection error. The saturation length is extracted from the evolution of the photon pulse energy along the undulator, defined as the position where the growth rate significantly decreases and the slope approaches zero. For each case, 12 simulations are performed with different shot noise. The given saturation length corresponds to the mean value, while the error bars indicate the standard error of the mean. A comparison between the two beamline configurations reveals a clear difference in their sensitivity to injection errors. At low errors, both configurations have comparable charge. However, the emittance is better preserved in the APL-based beamline, resulting in a shorter saturation length. The saturation length remains similar for both setups up to approximately 1.5 μrad . For larger injection errors, the performance of the PQMs-based beamline degrades more rapidly. As the injection error increases, a larger fraction of the beam is intercepted by the collimators. In particular, particles within the resonance window are lost more rapidly in the PQMs-based beamline, together with an increase in normalized emittance. These effects reduce the FEL gain and hinder the process.

Overall, the APL-based beamline shows greater tolerance to injection errors, maintaining saturation up to about 2.5 μrad due to better preservation of beam quality and higher transmission of resonant particles. In contrast, in the PQMs-based beamline the threshold is reached earlier, slightly below 2.0 μrad . This behavior is also reflected in Fig. 2, where the pulse energy evolution along the undulator is shown for each simulated injection error.

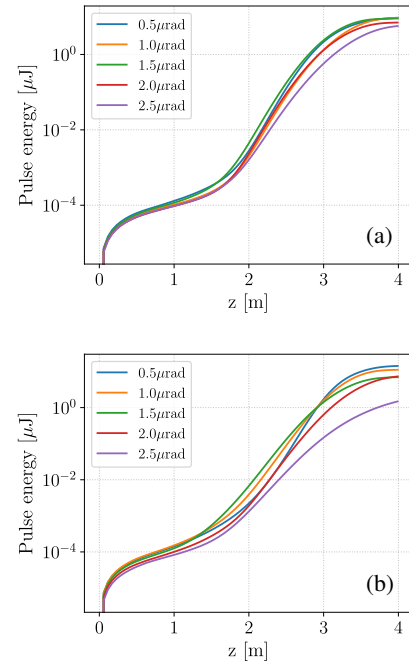


Figure 2: Pulse energy evolution along the undulator for the APL-based beamline (a) and for the PQMs-based beamline (b). For each injection error, the representative shot with saturation length closest to the mean value is displayed.

CONCLUSION

The results demonstrate that the choice of focusing system has a significant impact on the robustness of FEL operation. The APL-based beamline preserves beam quality more effectively and maintains higher transmission, allowing FEL saturation to be maintained at larger injection errors. In contrast, the PQMs-based beamline shows earlier degradation due to increased particle loss and higher emittance, which limits its operational tolerance. These findings highlight the advantage of the APL-based configuration for stable FEL performance under realistic conditions.

ACKNOWLEDGEMENTS

This work received funding from the European Union's Horizon Europe research and innovation program, under Grant Agreement No.101079773 (EuPRAXIA Preparatory Phase), No.101188004 (PACRI—Plasma Accelerator systems for Compact Research Infrastructures) and No.101073480 (EuPRAXIA Doctoral Network), and from the UKRI guarantee funds. This work was supported by the Swiss-Czech Research Infrastructure Initiative (project SWISSELITE, grant number 8K2501) financed by the Swiss-Czech Cooperation Programme. This work was supported by the Ministry of Education, Youth and Sports of the Czech Republic through the e-INFRA CZ (ID:90254)

I would also like to thank Sven Reiche for insightful discussions on GENESIS and Laury Batista for providing support with the TraceWin interface and technical issues.

REFERENCES

- [1] A. Molodozhentsev *et al.*, “Plasma accelerator based free electron laser program at ELI-ERIC (ELI-Beamlines)”, in *Proc. IPAC'24*, Nashville, TN, USA, May 2024, pp. 372–375. doi:10.18429/JACoW-IPAC2024-MOPG32
- [2] C. A. Lindstrøm *et al.*, “Emittance preservation in an aberration-free active plasma lens”, *Phys. Rev. Lett.*, 121.19, 194801, Nov. 2018. doi:10.1103/PhysRevLett.121.194801
- [3] T. Schmidt and S. Reiche, “Undulators for the SwissFEL”, in *Proc. FEL'09*, Liverpool, UK, Aug. 2009, paper THOA01, pp. 706–713.
- [4] K. Feng *et al.*, “High-quality electron beam generation from laser wakefield accelerators for driving compact free electron lasers”, *arXiv preprint arXiv:2501.09916*, Jan. 2025. doi:10.48550/arXiv.2501.09916
- [5] J. Zhan *et al.*, “Optimized laser wakefield acceleration: Generating stable, high-energy, monoenergetic electron beams and demonstrating extreme-ultraviolet free-electron lasers”, *Phys. Rev. Research* 8, p. 013207, 2026. doi:10.1103/qvg7-ng8n
- [6] R. A. Fonseca, *et al.*, “OSIRIS: A Three-Dimensional, Fully Relativistic Particle in Cell Code for Modeling Plasma Based Accelerators”, *Springer*, pp. 342–351, Berlin 2002. doi:10.1007/3-540-47789-6_36
- [7] Migliorati, Mauro, *et al.*, “Intrinsic normalized emittance growth in laser-driven electron accelerators”, *Phys. Rev. Lett. AB*, 16.1, Jan. 2013. doi:10.1103/PhysRevSTAB.16.011302
- [8] Li, Xiangkun, Antoine Chancé, and Phu Anh Phi Nghiem., “Preserving emittance by matching out and matching in plasma wakefield acceleration stage”, *Phys. Rev. Lett. AB*, 22.2, Feb. 2019. doi:10.1103/PhysRevAccelBeams.22.021304
- [9] S. K. Barber, C. B. Schroeder, J. van Tilborg, W. P. Leemans, “Transport and phase-space manipulation of laser-plasma accelerated electron beams using active plasma lenses”, *AIP Conf. Proc.*, March 2017. doi:10.1063/1.4975853
- [10] M. Miceski *et al.*, “Design of beam transport system integrating active plasma lens for laser-plasma driven EUV free-electron lasers”, in *Proc. IPAC'25*, Taipei, Taiwan, May 2025, pp. 110–113. doi:10.18429/JACoW-IPAC2025-MOPB022
- [11] J. Van Tilborg, *et al.*, “Comparative study of active plasma lenses in high-quality electron accelerator transport lines”, *Phys. Plasma*, 25, March 2018. doi:10.1063/1.5018001
- [12] A. Yu. Molodozhentsev and K. O. Kruchinin, “Compact LWFA-based extreme ultraviolet free electron laser: Design constraints”, *Instruments*, vol. 6, no. 1, p. 4, Jan. 2022. doi:10.3390/instruments6010004
- [13] D.Uriot, R.Duperrier and N.Pichoff, TraceWin, CEA Saclay, 2015. <https://www.dacm-logiciels.fr/tracewin>
- [14] S. Reiche, “GENESIS 1.3: a fully 3D time-dependent FEL simulation code”, *Nucl. Instrum. Methods Phys. Res., Sect. A*, 429.1-3, 1999, pp. 243–248. <https://github.com/svenreiche/Genesis-1.3-Version4>. doi:10.1016/S0168-9002(99)00114-X